Frontiers in Bioscience Landmark

Front. Biosci. (Landmark Ed) **2026**; 31(7): 50880
https://doi.org/10.31083/FBL50880

Original Research

MGST1 Suppresses Ferroptosis in Nucleus Pulposus Cells and Attenuates Intervertebral Disc Degeneration by Regulating GPX4

Zhenxin Huo[1,2,†], Ding Li[1,†], Yuxuan Kuang[1], Baoshan Xu[1,2,*]

[1]Department of Graduate School, Clinical College of Orthopedics, Tianjin Medical University, 300070 Tianjin, China
[2]Department of Minimally Invasive Spine Surgery, Tianjin Hospital, Tianjin University, 300211 Tianjin, China
*Correspondence: baoshanxu99@tmu.edu.cn (Baoshan Xu)
[†]These authors contributed equally.

Academic Editor: Elisa Belluzzi
Submitted: 9 February 2026 Revised: 20 April 2026 Accepted: 29 April 2026 Published: 24 July 2026

Abstract

Background: Intervertebral disc degeneration (IDD) is a major pathological contributor to low back pain, and its progression is closely associated with oxidative stress and cell death. Ferroptosis is a form of programmed cell death characterized by iron-dependent lipid peroxidation, which has recently been confirmed to participate in IDD progression. Microsomal glutathione S-transferase 1 (MGST1) plays an important role in glutathione metabolism and cellular antioxidant defense, but its function in IDD remains unclear. This study aimed to investigate the expression profile of MGST1 in IDD and to elucidate its molecular mechanism in delaying degeneration by regulating ferroptosis. **Methods:** Differentially expressed ferroptosis-related genes associated with intervertebral disc degeneration were screened through bioinformatics analysis. MGST1 expression changes were validated using a needle puncture-induced rat IDD model and a degenerated nucleus pulposus (NP) cell model. MGST1 knockdown and overexpression strategies were employed to evaluate its effects on the extracellular matrix metabolism, apoptosis, and senescence of nucleus pulposus cells. Further examinations of ferroptosis-related indicators were conducted, including levels of lipid peroxidation, reactive oxygen species generation, intracellular Fe^{2+} content, and changes in mitochondrial membrane potential. For *in vivo* experiments, the therapeutic effect of MGST1 overexpression was assessed by intradiscal injection of an MGST1-overexpressing lentivirus into the rat intervertebral disc degeneration model. **Results:** Bioinformatics analysis indicated that MGST1 is a key candidate gene in IDD. MGST1 expression was consistently upregulated with increasing degeneration severity in rat disc tissues and degenerated NP cells. Knockdown of MGST1 significantly promoted extracellular matrix degradation and increased apoptosis and senescence levels in NP cells, while MGST1 overexpression markedly improved these changes. Mechanistic studies revealed that MGST1 deficiency significantly enhanced ferroptosis characteristics in NP cells, including accumulation of lipid peroxides and ROS, increased Fe^{2+} content, and decreased mitochondrial membrane potential. In vivo experiments demonstrated that MGST1 overexpression significantly alleviated the degree of IDD in rats. **Conclusion:** MGST1 exhibits compensatory upregulation during the progression of intervertebral disc degeneration and delays its progression by inhibiting ferroptosis in nucleus pulposus cells. This study reveals a novel mechanism by which MGST1 regulates ferroptosis in IDD and provides a potential molecular target for the prevention and treatment of IDD.

Keywords: microsomal glutathione S-transferase 1; ferroptosis; intervertebral disc degeneration; nucleus pulposus cells

1. Introduction

Low back pain is one of the most common musculoskeletal disorders, and intervertebral disc degeneration (IDD) is considered a core pathological basis for its onset and progression [1,2]. Owing to the poor blood supply and low metabolic activity of disc tissue, the degenerative process is often progressive and difficult to reverse, and effective pharmacological interventions are still lacking. Therefore, elucidating the molecular mechanisms of IDD is of great significance.

The intervertebral disc consists of the nucleus pulposus (NP), annulus fibrosus, and cartilaginous endplates. NP cells play a key role in maintaining disc structure and biomechanical function [3]. During degeneration, the number of NP cells decreases, extracellular matrix (ECM) synthesis declines, with reduced levels of type II collagen and aggrecan. Catabolism-related proteins such as Matrix Metalloproteinases (MMPs) and A Disintegrin and Metalloproteinase with Thrombospondin Motifs (ADAMTS) are upregulated. Concurrently, enhanced apoptosis and senescence are considered important factors driving degeneration progression [4].

In recent years, the role of oxidative stress and related modes of cell death in IDD has garnered attention. Among these, ferroptosis is a novel form of cell death dependent on iron ions and characterized by lipid peroxidation [5]. Studies have shown that ferroptosis is activated in IDD, and its inhibition can, to some extent, protect NP cells [6,7]. However, the endogenous regulatory molecules of ferroptosis have not been fully elucidated.

Microsomal glutathione S-transferase 1 (MGST1) is involved in glutathione metabolism and lipid peroxide

Copyright: © 2026 The Author(s). Published by IMR Press.
This is an open access article under the CC BY 4.0 license.

Publisher's Note: IMR Press stays neutral with regard to jurisdictional claims in published maps and institutional affiliations.

clearance, playing an important role in maintaining cellular redox homeostasis [8], but its function in IDD remains unclear. This study combines bioinformatics with *in vitro* and *in vivo* experiments to systematically investigate the role of MGST1 in IDD and whether it participates in the disease process by regulating ferroptosis.

In a recent bioinformatic study, Huo et al. [9] analyzed the GSE70362 and GSE147383 datasets and identified MGST1 as a hub ferroptosis-related gene that was significantly upregulated in the degenerated annulus fibrosus. However, that study was primarily descriptive and did not investigate the functional role or regulatory mechanism of MGST1 in IDD. Whether MGST1 plays a protective role in NP cells—the key cell type maintaining disc homeostasis—and how it might regulate ferroptosis remain entirely unknown. Therefore, the present study aims to systematically characterize the functional significance of MGST1 in NP cells and elucidate its molecular mechanism in delaying IDD progression through ferroptosis inhibition.

2. Materials and Methods

2.1 Data Acquisition and Bioinformatics Analysis

The IDD-related transcriptome dataset GSE70362 was obtained from the GEO database (https://www.ncbi.nlm.nih.gov/geo/). Samples were divided into mild and moderate/severe degeneration groups based on the Thompson grading criteria. The R package 'limma' was used for data normalization and differential expression analysis to screen for significantly differentially expressed genes ($|\log2FC| > 1$, $p < 0.05$). The intersection of these DEGs with ferroptosis-related genes from the FerrDb database yielded candidate ferroptosis-related genes associated with IDD (http://www.zhounan.org/ferrdb/current/) [10], Further Gene Ontology (GO) functional annotation and KEGG pathway enrichment analyses were performed using the 'clusterProfiler' package.

2.2 Animal Experiments

2.2.1 Experimental Animals and Grouping

Sprague–Dawley (SD) rats (4 weeks old; Sbeifu Biotechnology Company, China) were used. Animals were randomly assigned into four groups: the sham group, needle puncture–induced degeneration group, needle puncture + LV-Vector group (lentiviral empty-vector control), and needle puncture + LV-MGST1 group (MGST1-overexpressing lentivirus). The lentivirus transfection reagent was purchased from ECM, No.: HY-K2015 China. Animals were housed in separate cages during the experiment, and general health status and mortality were monitored throughout the study.

2.2.2 Rat Caudal Disc Needle Puncture Model and Intradiscal Lentiviral Injection

Anesthesia. Prior to surgery, a 2% (w/v) sodium pentobarbital solution was prepared in sterile normal saline. Rats were weighed and anesthetized by intraperitoneal injection of sodium pentobarbital at 40 mg/kg. Surgical procedures were initiated after loss of spontaneous movement and nociceptive reflexes.

Disinfection. Rats were placed in the prone position and immobilized. The tail was exposed and the target caudal segments were marked. Routine disinfection with iodophor was performed, followed by sterile draping.

Needle puncture–induced degeneration. Under X-ray guidance, the Co6-Co7 intervertebral space was localized. A 27-G needle was inserted into the disc in a vertical direction, aligned with the intervertebral space. A needle holder was used to clamp the needle tip to restrict the puncture depth to approximately 1.5 mm. The needle was then rotated 180° along its axis, maintained in place for 30 s and subsequently withdrawn. In the sham group, only skin puncture for localization was performed.

Intradiscal injection. In the LV-Vector and LV-MGST1 groups, 2 µL of concentrated lentiviral suspension was first aspirated using a micropipette and then fully loaded into a microsyringe fitted with a 31-G needle (0.26 mm diameter), which is considerably finer than the 27-G needle (0.41 mm diameter) used for the initial needle puncture. Under X-ray guidance, the lentivirus was injected into the target intervertebral disc. Viral injections were initiated two weeks after model induction (i.e., when the rats were 6 weeks old) and were administered once weekly for a total of two injections (at weeks 2 and 3 post-induction). All animals were euthanized and disc tissues were harvested at 9 weeks of age (i.e., 5 weeks after model induction). The sham and needle puncture-only groups did not receive any viral injections.

Euthanasia. Rats were eut hanized via carbon dioxide (CO_2) inhalation. The CO_2 flow rate was set to 20% of the chamber volume per minute (approximately 3–5 L/min for a 15 L chamber), gradually displacing the air to achieve a final CO_2 concentration of 100%. Animals were exposed to the CO_2 atmosphere for at least 5 minutes after the cessation of spontaneous respiration. Death was confirmed by the absence of heartbeat and respiration for at least 2 minutes, and lack of response to a firm toe pinch. No additional physical or chemical methods were used.

2.3 Magnetic Resonance Imaging (MRI) and Histological Assessment

MRI. Rats were anesthetized according to the protocol described above (2% sodium pentobarbital, 40 mg/kg, intraperitoneal injection). Animals were positioned prone on the scanner bed with the limbs secured, and the tail was gently extended to remain straight. MRI was performed using a fast-spin echo sequence with a repetition time (TR) of 2000 ms and an echo time (TE) of 36 ms, a 256 (h) × 256 (v) matrix, a field of view (FOV) of 6.00/3.00 cm, and a flip angle of 180°. After MRI, animals were euthanized by CO_2 overdose, and caudal intervertebral disc tissues were harvested and fixed in 4% paraformaldehyde for 24–36 h.

Tissue processing and staining. After fixation, the rat tail was cut into segments. Samples were decalcified in 10% EDTA (pH 7.3) for 14 days (with the decalcification solution replaced every other day), followed by routine graded ethanol dehydration, xylene clearing, and paraffin embedding. Sections were stained with Safranin O–Fast Green, and the degree of disc degeneration was evaluated according to a histological scoring system.

2.4 NP Cell Isolation, Culture, and In Vitro Degeneration Model

SD rats aged 6–7 weeks were euthanized by CO_2 overdose, and caudal vertebrae were collected and disinfected with 75% ethanol for 3 min. Under sterile conditions, the skin was removed and the disc space was opened. Gelatinous NP tissues were carefully isolated and collected into sterile microcentrifuge tubes. Tissues were digested with 0.2% type II collagenase (Sangon Biotech, NO. A004174, China, diluted in serum-free DMEM/F12; the digestion volume was approximately fivefold the tissue volume) at 37 °C for approximately 4 h, with agitation every 30 min. After digestion, cells were centrifuged at 1000 rpm for 5 min, resuspended in complete DMEM/F12 (Solarbio Life Sciences, D6570, China) medium containing 5% fetal bovine serum (FBS, Oricell, FBSST-01033, China) and 1% penicillin/streptomycin (Sangon Biotech, NO. E607011, China), and cultured at 37 °C in 5% CO_2. Cells at passages 2–4 were used for subsequent experiments. All primary cells were validated for their identity by morphological observation and positive expression of COL2A1 and ACAN (Fig. 2), and tested negative for mycoplasma.

***In vitro* degeneration induction**. Tert-butyl hydroperoxide (TBHP, Aladdin, B106035, China) was used to establish an NP cell degeneration model. After dose-response screening, 50 μM TBHP for 24 h was selected as the standard degenerative condition.

2.5 MGST1 Knockdown/Overexpression and Ferroptosis Interventions

siRNA transfection. Transfection was performed when cells reached approximately 40% confluence. For each well of a 24-well plate, 1 μL siRNA was diluted in 50 μL Opti-MEM, and 2 μL RNAiMAX (IMAX, Lipofectamine 3000 Transfection Reagent, Invitrogen, L3000015, America) transfection reagent was diluted in 50 μL Opti-MEM. After standing at room temperature for 5 min, the two solutions were mixed and incubated for an additional 10 min, then added to the wells and gently mixed. Complete medium was replaced 24 h after transfection.

Plasmid transfection. Transfection was performed when cells reached approximately 70% confluence. For each well, 0.75 μg MGST1 overexpression plasmid (or empty vector) was diluted in 50 μL Opti-MEM, and 2.25 μL PolyFast transfection reagent was diluted in 50 μL Opti-MEM. After standing separately for 5 min, the solutions were mixed and incubated for 10 min, then added to cells. Medium was replaced 24 h after transfection.

Ferroptosis induction/inhibition. RSL-3 (a GPX4 inhibitor, MackLin, R798329, China) and Ferrostatin-1 (Fer-1; a ferroptosis inhibitor, MackLin, F792503, China) were dissolved in DMSO and diluted in complete medium. Cells were treated with 100 nM RSL-3 or 5 nM Fer-1 for 12 h. Control cells received an equal volume of DMSO.

2.6 Molecular and Cellular Assays

qRT-PCR. Total RNA was extracted using an Omega total RNA extraction kit (Omega, R6812-00S, America). Reverse transcription (TransGen Biotech, AE101-02, China) was performed at 50 °C for 5 min and 85 °C for 2 min. qPCR was conducted in a 10 μL reaction system under the following conditions: 94 °C for 30 s, followed by 40 cycles of 94 °C for 5 s, 56 °C for 15 s, and 72 °C for 10 s, with a final step of 92 °C for 5 min. Relative gene expression was calculated using the $2^{-\Delta\Delta Ct}$ method.

Western blotting. Cells were lysed on ice in RIPA (Beyotime, P0013B, China) buffer for 5 min and centrifuged at 10,000 rpm for 5 min to collect the supernatant. Samples were mixed with 5× loading buffer at a 4:1 ratio and boiled at 100 °C for 10 min. SDS-PAGE was performed at 80 V for ~30 min, then increased to 120 V until the bromophenol blue dye front reached the bottom of the gel. Proteins were transferred at a constant current of 300 mA for 1–2 h (on ice). Membranes were blocked with non-fat milk (yili, China) for 1 h, incubated with primary antibodies at 4 °C for 12–16 h, and then incubated with secondary antibodies at room temperature for 2 h before visualization and imaging.

Immunofluorescence. Cells were washed with PBS, fixed with 4% paraformaldehyde for 10 min, and permeabilized with 0.3% Triton X-100 for 3 min. Non-specific binding sites were blocked with 5% BSA. Cells were incubated with primary antibodies at 4 °C for 12–16 h, followed by FITC-conjugated secondary antibodies at room temperature for 2 h. Nuclei were counterstained using a DAPI-containing mounting medium. Images were acquired by confocal or fluorescence microscopy and quantified.

TUNEL and SA-β-gal assays. Apoptosis was assessed using a TUNEL kit (Beyotime, China, fixed with 4% paraformaldehyde for 10 min; permeabilized with 0.3% Triton X-100; TdT Enzyme:TRITC-dUTP = 1:9; incubation at 37 °C for 60 min in the dark). Cellular senescence was evaluated using an SA-β-gal staining kit (Beyotime, C1459S, China); cells were incubated at 37 °C overnight and then examined.

Ferroptosis-related functional assays.

① **ROS**: DCFH-DA (ECM, China) was diluted 1:1000 to a final concentration of 10 μM. 100 μL was added per well and incubated at 37 °C with 5% CO_2 for 20 min. Signals were detected using confocal microscopy (Olympus, Japan, excitation 488 nm; emission 525 nm).

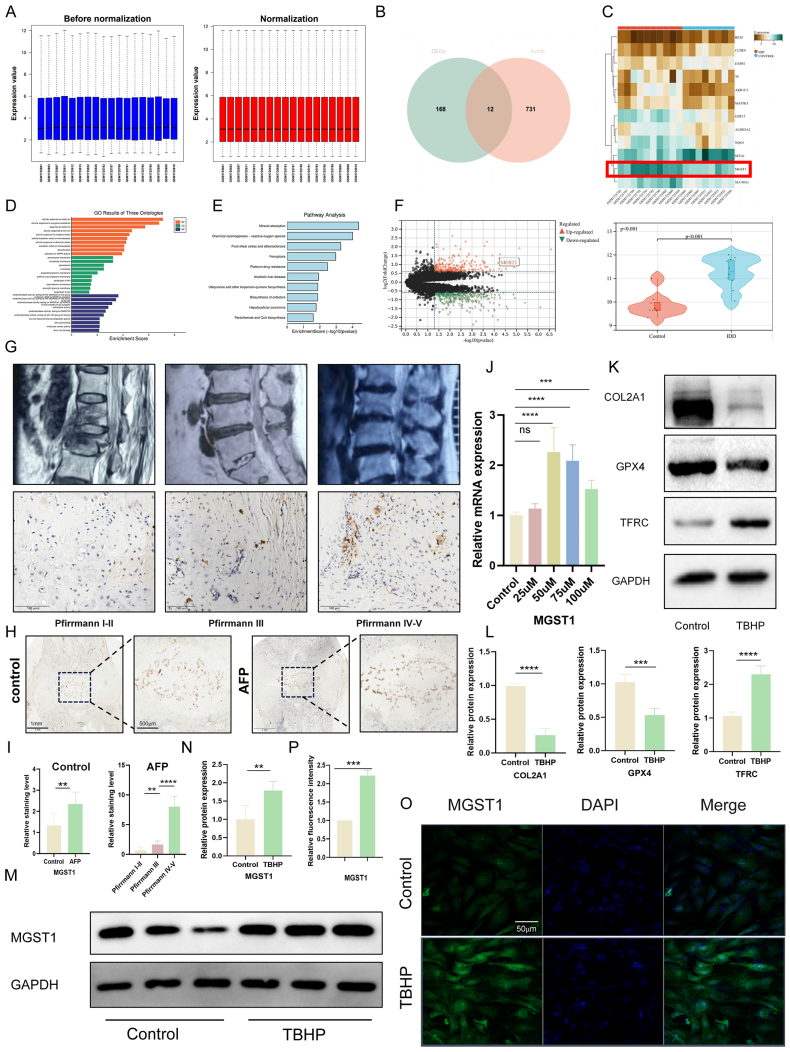

Fig. 1. MGST1 is identified as a key upregulated gene in intervertebral disc degeneration. (A) Differential gene results related to ferroptosis genes in GSE70362 and GO/KEGG enrichment analysis. Distribution of sample data before standardization (blue); distribution of sample data after standardization (red). (B) Intersection of 180 differential genes from GSE70362 and ferroptosis database genes yields 12 differential genes. (C) Heatmap of the 12 ferroptosis-related differential genes, with different color blocks representing different expression values. Green indicates high expression levels. The red box highlights the position of MGST1. (D,E) GO and KEGG analysis results of the 12 intervertebral disc degeneration-related differential genes, including MGST1. These differential genes are closely associated with regulatory pathways such as mineral absorption, reactive oxygen species, and ferroptosis. (F) Volcano plot of differential genes in GSE70362. (G) Intervertebral disc tissue was obtained from patients with lumbar spine trauma and classified as Pfirrmann grades I–V. Scale bar: 100 μm. (H) Immunohistochemical staining of MGST1 in intervertebral discs of normal rats and needle puncture-induced degeneration (AFP group) rat tails. Scale bars: 1 mm (main panel) and 500 μm (enlarged view). (I) Statistical analysis of rat immunohistochemistry and human intervertebral disc immunohistochemistry (**$p < 0.01$, ****$p < 0.0001$). (J) qRT-PCR shows changes in MGST1 expression in rat primary nucleus pulposus cells treated with TBHP at concentrations of 25 μM, 50 μM, 75 μM, and 100 μM for 24 hours. (K) Western Blot shows changes in the expression of extracellular matrix component COL2A1, ferroptosis protective marker GPX4, and transferrin TFRC in nucleus pulposus cells treated with TBHP. (L) Statistical and quantitative analysis results of Western Blot (ns: not significant, ***$p < 0.001$, ****$p < 0.0001$). (M–P) Western Blot and immunofluorescence staining show changes in MGST1 expression in nucleus pulposus cells treated with TBHP, along with statistical analysis (**$p < 0.01$, ***$p < 0.001$). Scale bar: 50 μm. MGST1, Microsomal glutathione S-transferase 1; GO, Gene Ontology; KEGG, Kyoto Encyclopedia of Genes and Genomes; AFP, Alpha-Fetoprotein; qRT-PCR, Quantitative Real-Time Reverse Transcription Polymerase Chain Reaction; TBHP, Tert-butyl hydroperoxide; COL2A1, Collagen Type II Alpha 1 Chain; GPX4, Glutathione Peroxidase 4; TFRC, Transferrin receptor protein 1.

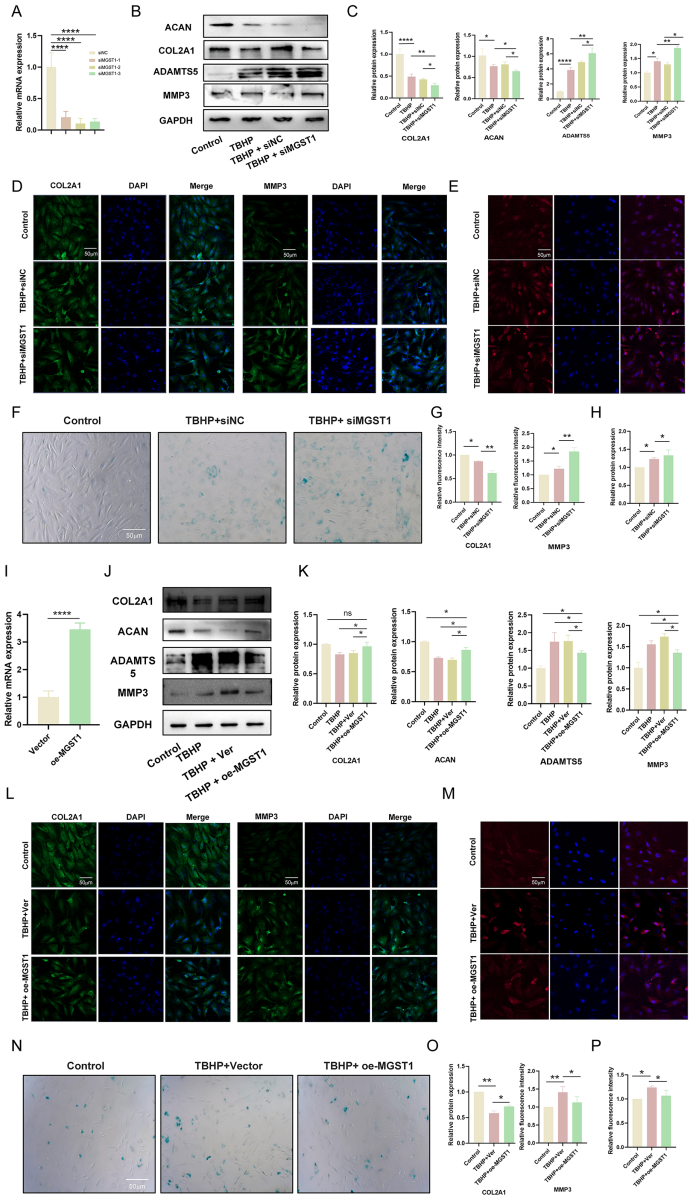

Fig. 2. MGST1 regulates extracellular matrix metabolism, apoptosis, and senescence in NP cells. (A) qRT-PCR shows that three different siRNAs significantly knockdown MGST1 expression in rat primary nucleus pulposus cells (****$p < 0.0001$). (B,C) Western Blot demonstrates the effect of MGST1 knockdown on the expression of extracellular matrix-related proteins in degenerated nucleus pulposus cells and quantitative analysis, including indicators such as COL2A1, ACAN, ADAMTS5, and MMP3 (*$p < 0.05$, **$p < 0.01$, ****$p < 0.0001$). (D,G) Immunofluorescence and quantitative analysis (*$p < 0.05$, **$p < 0.01$). Scale bar: 50 μm. (F) β-galactosidase staining shows the degree of senescence, with more pronounced green indicating higher senescence levels. Scale bar: 50 μm. (E,H) TUNEL staining displays the apoptosis level of nucleus pulposus cells and quantitative analysis, with more intense red indicating higher apoptosis levels (*$p < 0.05$). Scale bar: 50 μm. (I) qRT-PCR measures the transfection efficiency of the MGST plasmid (****$p < 0.0001$). (J,K) Western Blot and statistical analysis evaluate the expression levels of COL2A1, ACAN, ADAMTS5, and MMP3 upon overexpression of MGST1 (ns: not significant, *$p < 0.05$). (L,O) Immunofluorescence and statistical analysis assess the expression levels of COL2A1 and MMP3 upon overexpression of MGST1 (*$p < 0.05$, **$p < 0.01$). Scale bar: 50 μm. (N) β-galactosidase staining shows that the TBHP + oe-MGST1 group exhibits less green compared to the TBHP + Ver group. Scale bar: 50 μm. (M,P) TUNEL staining and quantitative analysis showed that the red fluorescence was weaker in the TBHP+oe-MGST1 group compared to the TBHP+Ver group. (P) Quantitative analysis of TUNEL staining (*$p < 0.05$). Scale bar: 50 μm. NP, nucleus pulposus; ACAN, Aggrecan; ADAMTS5, A Disintegrin And Metalloproteinase With Thrombospondin 5; MMP3, Matrix Metalloproteinase-3; TUNEL, Terminal deoxynucleotidyl Transferase-Mediated dUTP Nick End Labeling.

② **Fe^{2+}**: FerroOrange (ECM, HY-D0940, China) was prepared as a 1 μM working solution. After incubation at 37 °C, fluorescence was immediately observed under a fluorescence microscope without washing.

③ **Mitochondrial membrane potential**: JC-1 (ECM, HY-15534, China) staining working solution (100 μL per well) was incubated at 37 °C for 20 min; cells were washed twice and the red/green fluorescence ratio was analyzed.

④ **Lipid peroxidation**: Liperfluo (Beyotime, S0046S, China) was prepared as a 1 μM working solution; 100 μL per well was incubated at 37 °C for 30 min, followed by washing and fluorescence microscopy.

⑤ **CCK-8 assay**: 10 μL of CCK-8 solution (CCK-8 Assay Kit, Beyotime, C0037, China) was added to each well, incubated at 37 °C for 1 h, and absorbance was measured at 450 nm.

2.7 Statistical Analysis

All data are presented as mean ± standard deviation (SD) from three independent replicates (n = 3). Statistical analyses and figure generation were performed using GraphPad Prism 9. After testing homogeneity of variance, comparisons between two groups were conducted using Student's *t*-test. A value of $p < 0.05$ was considered statistically significant.

3. Results

3.1 MGST1 is Identified as a Key Upregulated Gene in Intervertebral Disc Degeneration

Differential analysis of the GSE70362 dataset identified multiple differentially expressed genes associated with IDD. Intersection with ferroptosis-related genes from the FerrDb database yielded 12 candidate genes, among which MGST1 was significantly upregulated in moderately to severely degenerated discs (Fig. 1A–C). GO and KEGG enrichment analyses revealed that these genes were primarily enriched in pathways related to oxidative stress response, iron ion metabolism, and lipid peroxidation (Fig. 1D,E). The volcano plot showed the overall distribution of differentially expressed genes (Fig. 1F).

MGST1 expression was progressively upregulated with increasing Pfirrmann grade in human degenerative disc tissues (Fig. 1G), and this trend was recapitulated in a rat tail needle-puncture-induced IDD model (Fig. 1H,I). Furthermore, in a TBHP-induced NP cell degeneration model, MGST1 expression was markedly upregulated under degenerative conditions (Fig. 1J–P).

3.2 MGST1 Regulates Extracellular Matrix Metabolism, Apoptosis, and Senescence in NP Cells

To investigate the function of MGST1 in NP cells, we performed siRNA-mediated knockdown and plasmid-mediated overexpression of MGST1 (Fig. 2A,I). Western Blot and Immunofluorescence results show that in both gain- and loss-of-function experiments, knocking down MGST1 significantly reduces the expression of collagen type II and aggrecan in NP cells, while promoting the upregulation of catabolic proteins such as MMP3 and ADAMTS5 (Fig. 2B–D,G). Conversely, MGST1 overexpression effectively maintained the synthesis levels of extracellular matrix components (Fig. 2J–L,O).

TUNEL staining indicated that MGST1 knockdown significantly increased the proportion of apoptotic NP cells, whereas MGST1 overexpression notably suppressed apoptosis (Fig. 2E,H,M,P). β-galactosidase staining further demonstrated that MGST1 deficiency promoted NP cell senescence, while MGST1 overexpression exerted a significant inhibitory effect on cellular senescence (Fig. 2F,N).

3.3 MGST1 Protects NP Cells by Inhibiting Ferroptosis

To further explore the mechanism of MGST1, we knocked down MGST1 in NP cells and assessed ferroptosis-related indicators (Fig. 3B,C). Functional assays related to ferroptosis revealed that MGST1 knockdown significantly increased intracellular ROS levels (Fig. 3F,G), lipid peroxide accumulation (Fig. 3J,K), and Fe^{2+} content (Fig. 3H,I), and led to a decrease in mitochondrial membrane potential (Fig. 3L), indicating enhanced ferroptosis (Fig. 3A–K).

Western blot and immunofluorescence results showed that MGST1 deficiency was accompanied by decreased GPX4 expression and aberrant changes in other ferroptosis-related proteins such as SLC7A11 and TFRC (Fig. 3B,D). Co-treatment with the ferroptosis inhibitor Ferrostatin-1 partially reversed the cellular damage caused by MGST1 knockdown, further supporting the protective role of MGST1 in suppressing ferroptosis.

3.4 MGST1 Attenuates Ferroptosis Through GPX4-Related Regulation

Based on STRING database analysis, we predict that MGST1 may mediate its anti-ferroptosis effect by targeting GPX4, a key regulator of ferroptosis (Fig. 4A). This was subsequently validated through Co-IP experiments, which confirmed that MGST1 can directly bind to GPX4 (Fig. 4B,C). Rescue experiments showed that under conditions of ferroptosis induced by the GPX4 inhibitor RSL-3, overexpression of MGST1 could still partially restore GPX4 expression and suppress changes in ferroptosis markers (Fig. 4D,E). These findings suggest that MGST1 suppresses ferroptosis in nucleus pulposus cells, potentially through a GPX4-associated mechanism.

3.5 MGST1 Attenuates Intervertebral Disc Degeneration In Vivo

To validate the protective role of MGST1 *in vivo*, we established a rat tail disc needle-puncture degeneration model and administered intradiscal injections of either LV-Vector or LV-MGST1 lentivirus (Fig. 5A,C). After two weeks of intradiscal injections, MRI analysis revealed that

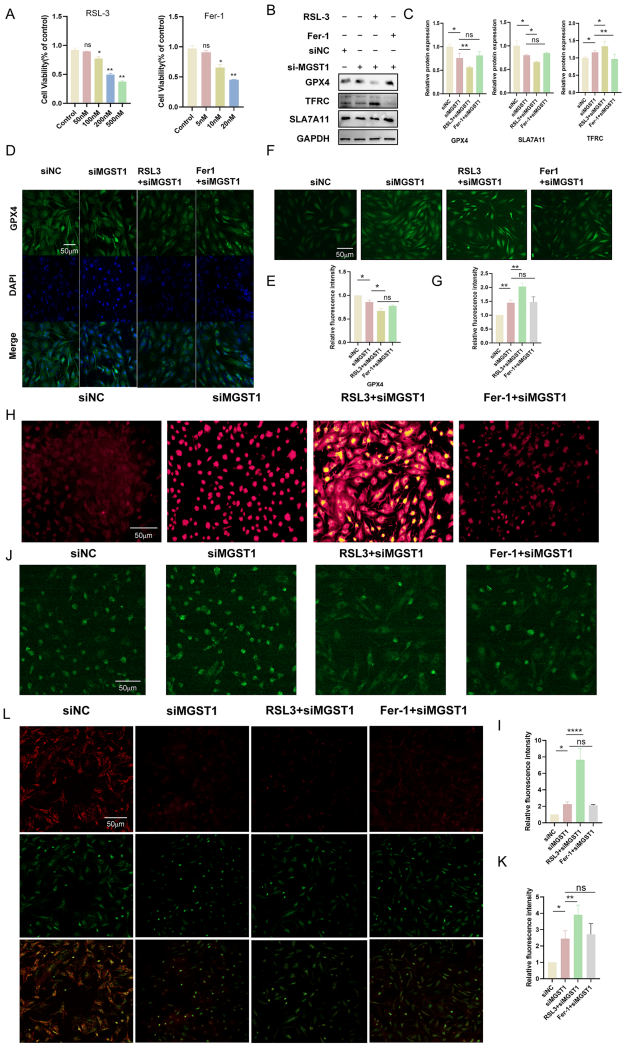

Fig. 3. MGST1 protects NP cells by inhibiting ferroptosis. (A) CCK-8 assay shows the effects of different concentrations of treatment agents on nucleus pulposus cell viability. RSL-3 induces ferroptosis in nucleus pulposus cells and specifically inhibits GPX4 expression. Cell viability significantly decreases when treated with 200 nM RSL-3 for 12 hours (ns: not significant, *$p < 0.05$, **$p < 0.01$). Fer-1 inhibits the progression of ferroptosis in nucleus pulposus cells, and this drug significantly affects nucleus pulposus cell viability at a concentration of 10 nM. (B–E) Western Blot and immunofluorescence show that knockdown of MGST1 promotes ferroptosis in nucleus pulposus cells (ns: not significant, *$p < 0.05$, **$p < 0.01$). Scale bar: 50 μm. (F,G) ROS fluorescent probe detects changes in ROS levels. The RSL3 + siMGST1 group shows increased ROS levels compared to the siMGST1 group, while the Fer-1 + siMGST1 group shows no statistically significant difference compared to the siMGST1 group (ns: not significant, **$p < 0.01$). Scale bar: 50 μm. (H,I) Fe^{2+} fluorescent probe detects Fe^{2+} levels. The Fer-1 + siMGST1 group shows no significant change in Fe^{2+} content compared to the siMGST1 group, while the RSL3 + siMGST1 group shows a significant increase in Fe^{2+} content compared to the siMGST1 group (ns: not significant, *$p < 0.05$, ****$p < 0.0001$). Scale bar: 50 μm. (J,K) Liperfluo cellular lipid peroxidation probe. The Fer-1 + siMGST1 group shows no statistically significant difference in lipid peroxidation content compared to the siMGST1 group, while the RSL3 + siMGST1 group shows a significant increase in lipid peroxidation content compared to the siMGST1 group (ns: not significant, *$p < 0.05$, **$p < 0.01$). Scale bar: 50 μm. (L) JC-1 probe detects mitochondrial outer membrane potential in each group. Compared to the siMGST1 group, the Fer-1 + siMGST1 group shows a reduction in mitochondrial outer membrane potential, and the RSL3 + siMGST1 group shows a significant reduction in mitochondrial outer membrane potential compared to the siMGST1 group, which is significantly lower than that of the siNC group. Scale bar: 50 μm. CCK-8, Cell Counting Kit-8; RSL-3, RAS-Selective Lethal 3; ROS, Reactive Oxygen Species; JC-1, JC-1 staining for mitochondrial membrane potential (ΔΨm) assessment. Representative fluorescence images show JC-1 aggregates (red) and monomers (green) in each group. The red/green fluorescence intensity ratio reflects the mitochondrial membrane potential. Scale bar: 50 μm.

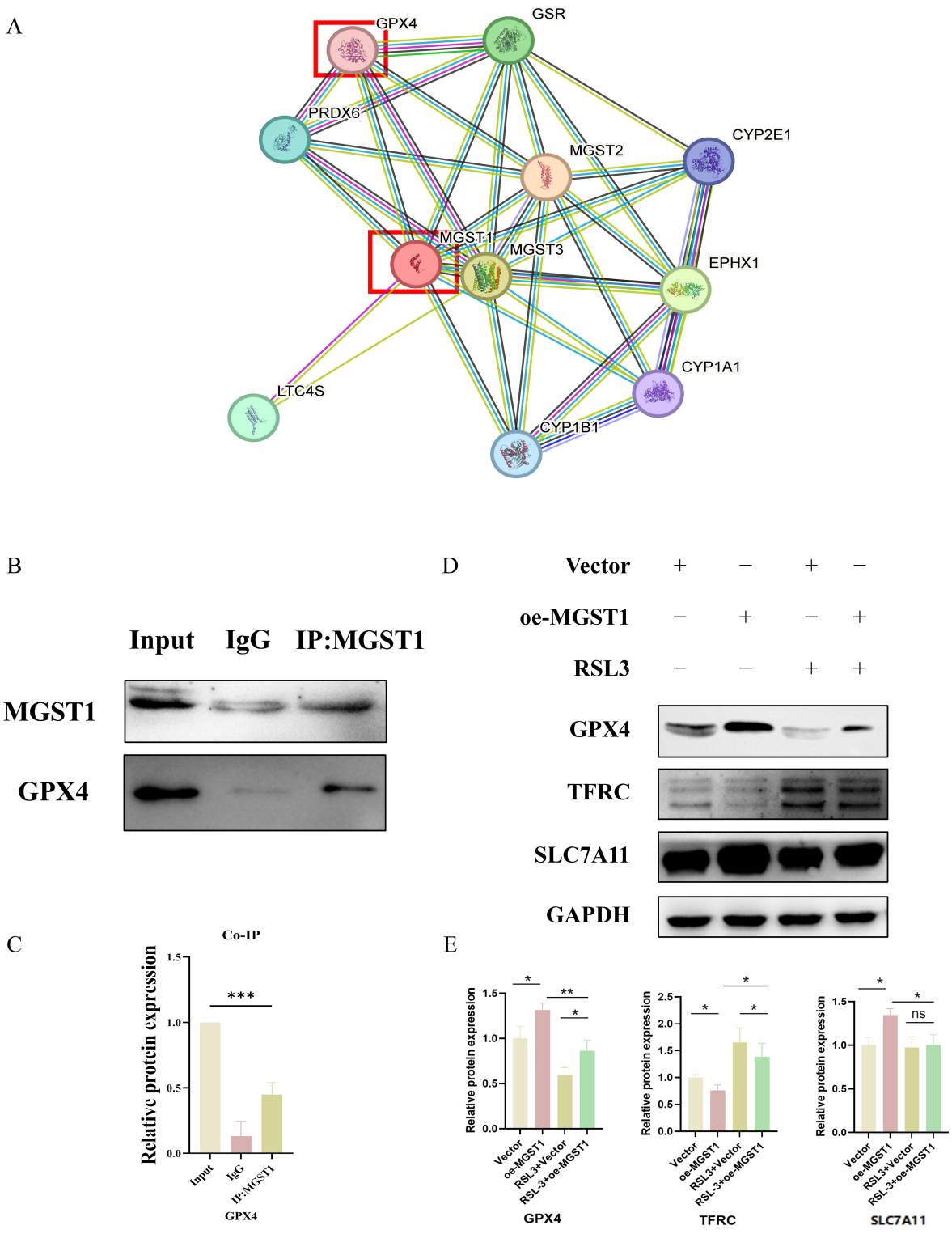

Fig. 4. MGST1 exerts anti-ferroptotic effects by targeting GPX4. (A) From the protein-protein interaction prediction network of the STRING database, MGST1 is predicted to bind with GPX4. (B,C) Co-IP experiments demonstrated that MGST1 can directly bind to GPX4. (D,E) Western Blot and statistical analysis were performed to detect the ferroptosis-related indicators GPX4, TFRC, and SLC7A11 after overexpressing MGST1 and treating with the GPX4 inhibitor RSL3. (ns: *not significant*, *$p < 0.05$, **$p < 0.01$, ***$p < 0.001$).

the LV-MGST1 group exhibited a significantly lower degree of disc degeneration (Pfirrmann grade) compared to the control group. Histological analysis via Safranin O/Fast Green staining further confirmed that the LV-MGST1 group maintained more intact disc structure and showed significantly improved histological scores (Fig. 5B,D). These results indicate that intradiscal overexpression of MGST1 effectively delays the progression of intervertebral disc degeneration in rats.

3.6 MGST1 Attenuates Intervertebral Disc Degeneration by Inhibiting Ferroptosis in Nucleus Pulposus Cells via GPX4 Activation

To further elucidate the protective mechanism of MGST1 in IDD, a schematic diagram was generated based on the experimental findings (Fig. 6). As shown, extracellular oxidative stress (TBHP) acts on NP cells, leading to a compensatory upregulation of MGST1 (↑). MGST1 then targets and activates GPX4, promoting its stabilization and activity. Activated GPX4 effectively suppresses ferroptosis, as evidenced by reduced lipid peroxidation, decreased ROS levels, and lower Fe^{2+} content. The inhibition of ferroptosis protects extracellular matrix (ECM) metabolism in NP cells, with increased COL2A1 and ACAN expression and decreased MMP3 and ADAMTS5 expression. Additionally, NP cell apoptosis and senescence are significantly reduced. Within the nucleus, transcriptional regulation of ECM-related genes (COL2A1, ACAN, MMP3, ADAMTS5) contributes to this protective process. Collectively, these effects delay the progression of IDD. The dashed green arrow indicates the overall protective effect mediated by the MGST1–GPX4 axis.

4. Discussion

This study systematically elucidated the expression pattern of MGST1 in IDD and its molecular mechanism in delaying degeneration progression through regulating ferroptosis. Specifically, we demonstrate that MGST1 regulates multiple signaling pathways involved in intervertebral disc degeneration, including the ferroptosis pathway, the GPX4-mediated anti-oxidant defense axis, and the ECM metabolic network. The results showed that MGST1 was significantly upregulated in rat degenerated disc tissues and degenerated NP cells. Functional experiments further confirmed that MGST1 overexpression could alleviate extracellular matrix breakdown, inhibit apoptosis and senescence, thereby maintaining NP cell homeostasis. This suggests that the high expression of MGST1 is more likely a compensatory upregulation rather than mere pathological activation, but whether this endogenous upregulation exerts a functional protective effect requires further investigation.

MGST1 belongs to the membrane-associated proteins in eicosanoid and glutathione metabolism (MAPEG) family and plays an important role in clearing lipid peroxides and regulating redox homeostasis [8]. Previous research has focused on its antioxidant functions in diseases such as tumor drug resistance and ischemic-hypoxic injury, while its role in IDD remained unclear. This study fills this gap, revealing that MGST1 may be an important molecular regulatory node in maintaining the intradiscal microenvironmental stability.

Ferroptosis, as a novel form of programmed cell death proposed in recent years, has gradually gained attention in IDD [11]. Characterized by iron accumulation and enhanced lipid peroxidation, ferroptosis can amplify oxidative stress and disrupt cell membrane stability. This study found that under degenerative conditions, ferroptosis in NP cells was markedly activated, and ferroptosis inhibitors could alleviate cellular damage, further supporting the involvement of ferroptosis in the IDD process [12].

More importantly, this study mechanistically revealed the direct link between MGST1 and ferroptosis. Based on bioinformatic prediction and pharmacological perturbation of GPX4, our data support that MGST1 may modulate GPX4-related anti-ferroptotic defense; notably, GPX4 is a central enzyme that limits lipid peroxidation and thereby constrains ferroptosis [13]. When MGST1 was knocked down, GPX4 expression decreased, and ferroptosis characteristics were significantly enhanced; conversely, MGST1 overexpression effectively mitigated these changes. This indicates that the MGST1–GPX4 axis is an important endogenous defense pathway regulating ferroptosis in NP cells, providing new molecular evidence for the involvement of ferroptosis in IDD.

In vivo experiments further demonstrated that MGST1 overexpression significantly improved structural degeneration in rat intervertebral discs, suggesting its potential translational value. It should be noted that exogenous overexpression experiments demonstrate that ‘an increased level of MGST1 protein is sufficient to confer a protective effect’, whereas whether endogenous upregulation plays a similar role under physiological or pathological conditions typically requires validation using gene knockout or knockdown models under stress conditions. In this study, siRNA knockdown experiments have shown that loss of endogenous MGST1 exacerbates degeneration, providing indirect support for the protective role of endogenous MGST1 (including its upregulated fraction). However, to rigorously prove that ‘endogenous upregulation during degeneration itself’ has a functional protective effect, the ideal experimental design would involve conditional inducible knockout models or the use of specific inhibitors to block stress-induced MGST1 upregulation while maintaining basal expression levels. We have listed this as an important direction for future research.

This study has several limitations. First, although we observed a progressive upregulation of MGST1 in degenerated disc tissues and NP cells, the functional role of this endogenous upregulation remains to be directly validated. Our experiments demonstrated that exogenous MGST1

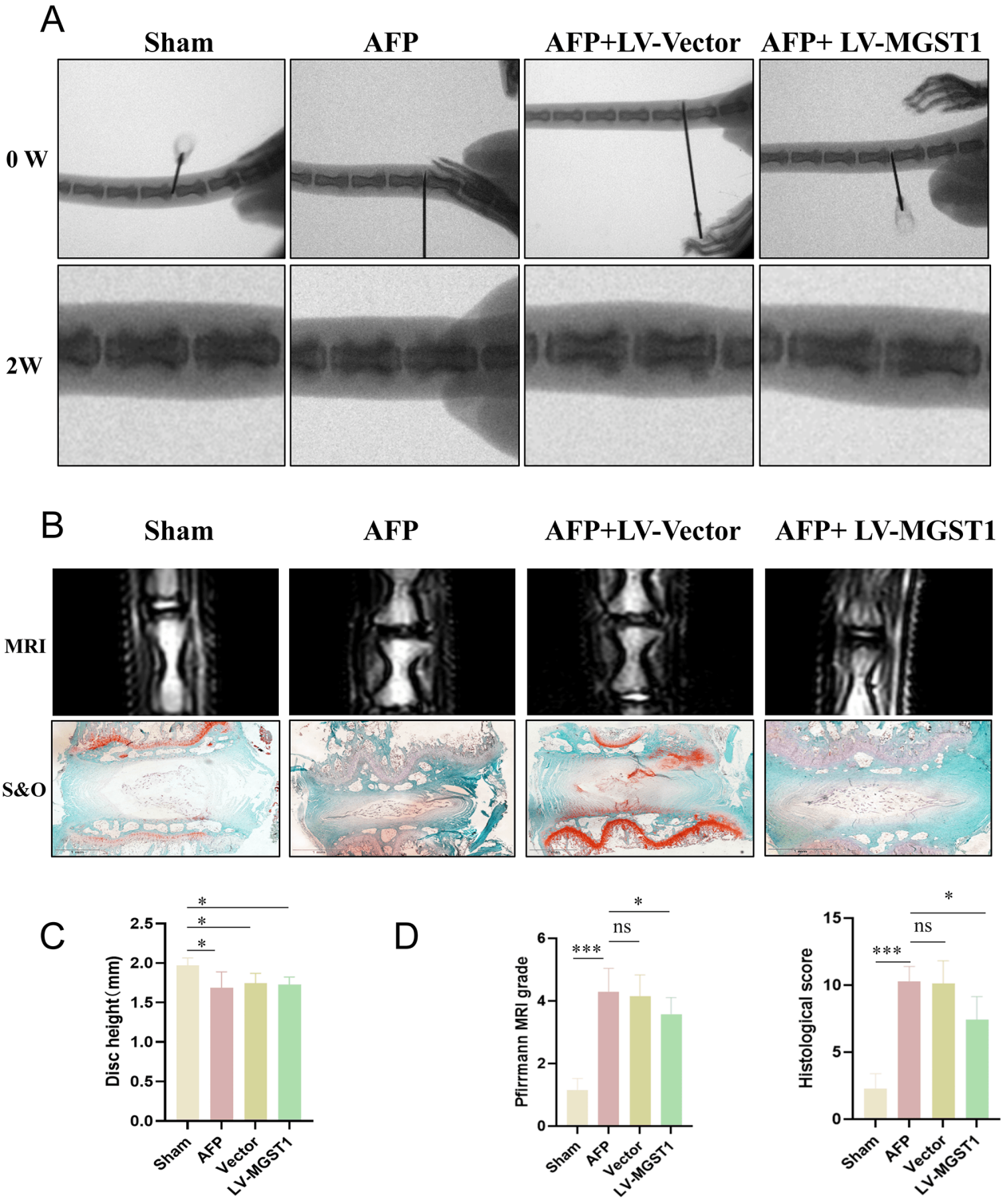

Fig. 5. MGST1 attenuates intervertebral disc degeneration *in vivo*. (A,C) X-ray examination and statistical analysis of the needle-induced intervertebral disc degeneration model in rat tails. Compared to the sham-operated group, disc height decreased in the needle-induced degeneration group, needle + LV-Vector group, and needle + LV-MGST1 group (AFP: needle-induced degeneration group; $*p < 0.05$). (B,D) Representative T2-weighted MRI images, safranin O-fast green staining, and statistical analysis of the sham-operated group, needle-induced degeneration group, needle + LV-Vector injection group, and needle + LV-MGST1 injection group (ns: not significant, $*p < 0.05$, $***p < 0.001$). Scale bar = 1 mm.

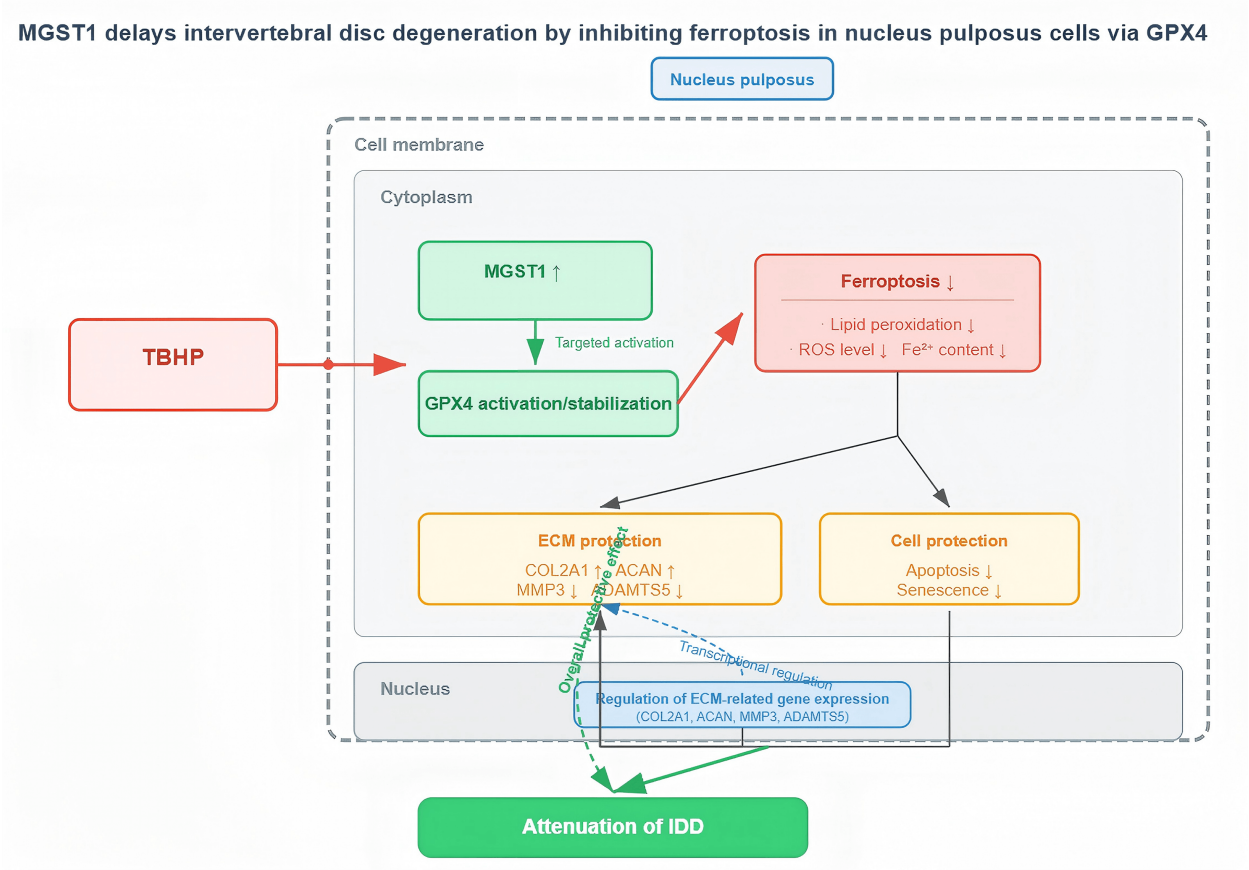

Fig. 6. MGST1 attenuates intervertebral disc degeneration by inhibiting ferroptosis in nucleus pulposus cells via GPX4 activation. Upregulation of MGST1 promotes GPX4 activation, suppresses ferroptosis, restores ECM homeostasis, reduces apoptosis/senescence, and attenuates IDD. Figure was created using BioRender (https://biorender.com/).

overexpression exerts protective effects, but whether the naturally occurring increase in MGST1 during degeneration serves a compensatory protective function requires further investigation, such as conditional knockout or specific blockade of stress-induced upregulation. Second, our mechanistic experiments used Fer-1 as a specific ferroptosis inhibitor to rescue MGST1 knockdown-induced phenotypes; while Fer-1 is widely accepted in the field, complementary genetic evidence (e.g., GPX4 overexpression) was not provided, which would have further strengthened the causal link between MGST1 and the GPX4-ferroptosis axis. Third, our animal model employed 4-week-old rats, whose intervertebral discs are predominantly composed of notochordal cells and stem cells, differing from the chondrocyte-like cells in adult human discs. Although this model is suitable for initial mechanistic studies, the findings should be extrapolated to human IDD with caution, and validation in adult or human-derived cells is needed. Fourth, the intradiscal injection protocol involved two weekly lentiviral injections (using a 31-G needle, which has a much smaller diameter (0.26 mm) than the 27-G needle (0.41 mm) used for the initial puncture), starting two weeks after model induction. Although this approach was balanced between treatment groups and ensured sustained MGST1 overexpression for proof-of-concept purposes, it does not reflect any clinically applicable regimen and may have introduced some additional needle injury beyond the initial puncture. However, the use of a finer needle for injections minimized the cumulative damage. Future studies should explore single-injection strategies using more efficient vectors (e.g., AAV) or sustained-release systems. Fifth, our *in vitro* and *in vivo* analyses focused primarily on NP cells; the role of MGST1 in annulus fibrosus and endplate cells remains unexplored. Sixth, among ECM-degrading enzymes, we assessed ADAMTS5 and MMP3 but did not examine ADAMTS4 or MMP-13, both of which are highly relevant to IDD. Finally, the upstream regulatory mechanisms and the precise temporal pattern of MGST1 upregulation during degeneration have not been elucidated. These limitations should be considered when interpreting the results, and addressing them will be an important direction for future research.

In summary, this study systematically reveals for the first time the molecular mechanism by which MGST1 delays IDD through regulating ferroptosis. It proposes that the MGST1–GPX4–ferroptosis axis is an important defense

system for maintaining NP cell homeostasis, providing a new theoretical basis and potential therapeutic target for the prevention and treatment of IDD.

5. Conclusion

MGST1 delays the progression of intervertebral disc degeneration by targeting GPX4 to inhibit ferroptosis in nucleus pulposus cells. This study not only expands the molecular regulatory network of ferroptosis in IDD but also provides a new theoretical basis and potential intervention strategy for the prevention and treatment of IDD-related diseases.

Availability of Data and Materials

The datasets analysed during the current study are available in the GEO database (https://www.ncbi.nlm.nih.gov/geo/) and FerrDb (http://www.zhounan.org/ferrdb/current/), which is an updated and openly accessible resource. Additional data and materials supporting the findings of this study are available from the corresponding author upon request.

Author Contributions

ZH performed the experiments, collected and analyzed the data, and wrote the original draft. DL performed experiments, data curation, statistical analysis, and software validation. YK participated in the investigation and validation of the results. BX conceived and supervised the study, acquired funding, and revised the manuscript. All authors contributed to editorial changes in the manuscript. All authors read and approved the final manuscript. All authors have participated sufficiently in the work and agreed to be accountable for all aspects of the work.

Ethics Approval and Consent to Participate

The animal experiment of the study was approved by the Tianjin Hospital (No.DXVTT-IACUC-20241016). All animal procedures were performed in accordance with the ARRIVE guidelines 2.0 and the Chinese national standard "Guideline for ethical review of animal welfare" (GB/T 35892-2018).

Acknowledgment

We thank all contributors to the GEO database. We thank the support of the Tianjin Hospital for providing the necessary ethical approval for this research.

Funding

This work was supported by the National Natural Science Foundation of China (No. 82472494).

Conflicts of Interest

The authors declare no conflicts of interest.

Supplementary Material

Supplementary material associated with this article can be found, in the online version, at https://doi.org/10.31083/FBL50880.

References

[1] The Lancet Rheumatology. The global epidemic of low back pain. The Lancet. Rheumatology. 2023; 5: e305. https://doi.org/10.1016/S2665-9913(23)00133-9

[2] GBD 2021 Low Back Pain Collaborators. Global, regional, and national burden of low back pain, 1990-2020, its attributable risk factors, and projections to 2050: a systematic analysis of the Global Burden of Disease Study 2021. The Lancet. Rheumatology. 2023; 5: e316–e329. https://doi.org/10.1016/S2665-9913(23)00098-X

[3] Waxenbaum JA, Reddy V, Williams C, Futterman B. Anatomy, Back, Lumbar Vertebrae. In StatPearls. 2026.

[4] Zhong H, Zhou Z, Guo L, Liu F, Zheng B, Bi S, et al. The miR-623/CXCL12 axis inhibits LPS-induced nucleus pulposus cell apoptosis and senescence. Mechanisms of Ageing and Development. 2021; 194: 111417. https://doi.org/10.1016/j.mad.2020.111417

[5] Dixon SJ, Lemberg KM, Lamprecht MR, Skouta R, Zaitsev EM, Gleason CE, et al. Ferroptosis: an iron-dependent form of nonapoptotic cell death. Cell. 2012; 149: 1060–1072. https://doi.org/10.1016/j.cell.2012.03.042

[6] Jia C, Xiang Z, Zhang P, Liu L, Zhu X, Yu R, et al. Selenium-SelK-GPX4 axis protects nucleus pulposus cells against mechanical overloading-induced ferroptosis and attenuates senescence of intervertebral disc. Cellular and Molecular Life Sciences: CMLS. 2024; 81: 49. https://doi.org/10.1007/s00018-023-05067-1

[7] Li C, Zhang Y, Deng Y, Chen Y, Wu C, Zhao X, et al. Fisetin suppresses ferroptosis through Nrf2 and attenuates intervertebral disc degeneration in rats. European Journal of Pharmacology. 2024; 964: 176298. https://doi.org/10.1016/j.ejphar.2023.176298

[8] Hayes JD, Flanagan JU, Jowsey IR. Glutathione transferases. Annual Review of Pharmacology and Toxicology. 2005; 45: 51–88. https://doi.org/10.1146/annurev.pharmtox.45.120403.095857

[9] Huo Z, Li D, Zhang K, Yan B, Zhang T, Li Z, et al. MGST1 May Regulate the Ferroptosis of the Annulus Fibrosus of Intervertebral Disc: Bioinformatic Integrated Analysis and Validation. Frontiers in Bioscience (Landmark Edition). 2024; 29: 224. https://doi.org/10.31083/j.fbl2906224

[10] Zhou N, Yuan X, Du Q, Zhang Z, Shi X, Bao J, et al. FerrDb V2: update of the manually curated database of ferroptosis regulators and ferroptosis-disease associations. Nucleic Acids Research. 2023; 51: D571–D582. https://doi.org/10.1093/nar/gkac935

[11] Yang RZ, Xu WN, Zheng HL, Zheng XF, Li B, Jiang LS, et al. Involvement of oxidative stress-induced annulus fibrosus cell and nucleus pulposus cell ferroptosis in intervertebral disc degeneration pathogenesis. Journal of Cellular Physiology. 2021; 236: 2725–2739. https://doi.org/10.1002/jcp.30039

[12] Fan C, Chu G, Yu Z, Ji Z, Kong F, Yao L, et al. The role of ferroptosis in intervertebral disc degeneration. Frontiers in Cell and Developmental Biology. 2023; 11: 1219840. https://doi.org/10.3389/fcell.2023.1219840

[13] Yang WS, SriRamaratnam R, Welsch ME, Shimada AF, Skouta CB, Viswanathan LM, et al. Regulation of ferroptotic cancer cell death by GPX4. Cell. 2014; 156: 317–331. https://doi.org/10.1016/j.cell.2013.12.010